Article

Analysis of the Characteristics of Uneven Spatio-Temporal Distribution in Wujiang River Basin over the Last 60 Years

Junchao Wang [1,2]**, Tao Peng** [1,2,3,]*****, Yiheng Xiang** [1,2,3]**, Zhiyuan Yin** [1,2,3] **and Haixia Qi** [1,2]

[1] China Meteorological Administration Basin Heavy Rainfall Key Laboratory/Hubei Key Laboratory for Heavy Rain Monitoring and Warning Research, Institute of Heavy Rain, China Meteorological Administration, Wuhan 430205, China; wjc@whihr.com.cn (J.W.); yiheng@whihr.com.cn (Y.X.); yinzy@whihr.com.cn (Z.Y.); haixiaqi@whihr.com.cn (H.Q.)

[2] Three Gorges National Climatological Observatory, Yichang 443099, China

[3] Hubei Key Laboratory of Intelligent Yangtze and Hydroelectric Science, China Yangtze Power Co., Ltd., Yichang 443000, China

***** Correspondence: pt_mail@whihr.com.cn

Abstract: Exploring the characteristics of uneven temporal and spatial distribution of precipitation in mountain watersheds can provide a reference for regional agricultural development and resource utilization, and contribute to the protection of the ecological environment. Based on the daily precipitation observation data of 40 meteorological stations in the Wujiang River Basin from 1963 to 2021, the temporal- and spatial-variation characteristics of the precipitation concentration degree (PCD) and precipitation concentration period (PCP) were analyzed using the Randall S analysis method, Mann–Kendall test method, Pettitt method, wavelet analysis and empirical orthogonal function (EOF). The results showed that the fluctuation range of PCD in Wujiang River Basin from 1963 to 2021 was 0.34–0.59, with a multi-year average of 0.47, which was obviously higher than the national average level and is showing a trend of slowly increasing. The fluctuation range of PCP was between 17.1 and 21.5 days, with a multi-year average of 19.0. The annual precipitation was mostly concentrated around the middle of July and showed a slowly decreasing trend. The abrupt change in PCD and PCP occurred around 1983 and 2001, respectively. There is an obvious Hearst phenomenon in PCP. In the future, the trend of precipitation concentration in the middle period will remain in advance, and the degree of precipitation concentration will continue to increase. The maximum precipitation in the flood season will continue to be delayed. The spatial pattern of the first mode of PCD and PCP in the Wujiang River basin was consistent and showed an opposite pattern between the upper reaches and the middle-lower reaches of the basin, which reflects the influence of the topography of the basin on the spatial distribution of precipitation. The distribution of precipitation is affected by topography. The elevation change in the basin was complex, and the leeward slope varied a lot. Therefore, it has a significant impact on precipitation. Areas with less precipitation are at higher elevations and on mountain leeward slopes, with a lack of moist air flow. The area with more precipitation was the summer monsoon mountain windward slope, and the topography blocks the increase in precipitation. The elevation of the central region is relatively uniform and the terrain is flat. Therefore, the distribution of precipitation is more uniform.

Keywords: Wujiang River; Mann–Kendall; characteristics; wavelet analysis

1. Introduction

Global warming not only directly affects the extreme change in air temperature, but also the change in global hydrological cycle. It is characterized by the redistribution and adjustment of regional precipitation, including the intensity of precipitation, the non-stationarity of precipitation concentration and so on. As a result, there are anomalies of extreme hydrological events, which lead to the aggravation of drought and flood disasters [1–3]. The sixth assessment report of IPCC, Climate change 2021: the Foundation of

Natural Science, was released in 2021, which reveals that human activities have caused the climate to warm at an unprecedented rate. Every region is facing more and more changes. Extreme heat and rainfall events have become more frequent. The Climate change 2023 report stresses that human activities have led to global warming and that extreme weather events have become more frequent and intense. Stronger heat waves, stronger rainfall and other extreme weather have further increased, posing significant risks to human health and ecosystems. The above challenges have further prompted the scientific community to conduct in-depth research on climate change in order to deepen global understanding of climate change. The stationarity assumption of hydrological series is the basic assumption of traditional hydrostatical methods in the analysis and study of hydrological series. With the influence of climate change and human activities on surface hydrological processes, this assumption is often problematic, which leads to misleading conclusions in hydrological analysis. Koutsoyiannis studied Climate change, the Hurst phenomenon, and hydrological statistics [4]. He found that there is an obvious trend of hydrological series in a short period of time being observed in a longer period of time. Hydrological statistics, the branch of hydrology that deals with uncertainty, in its current state is not consistent with the varying character of climate. Different time scales have been used to study precipitation concentration, including the monthly scale, weather scale, daily scale and so on. Fabio employed the K-means algorithm to divide Veneto into nine homogeneous regions, each characterized by specific evapotranspiration and climatic features. Furthermore, the seasonal Mann–Kendall (MK) test and the innovative trends analysis (ITA) method were used to investigate the trends related to monthly precipitation, ETo, and climate variables [5]. Stefanos collected and analyzed long-term (1961–2016) monthly rainfall data from nine rain gauges. Seasonal and annual rainfall data were subjected to Mann–Kendall tests to assess the possible upward or downward statistically significant trends, and to change-point analyses to detect whether a change in the rainfall time series mean had taken place [6]. CHAUAN investigated the spatio-temporal distribution of rainfall and rain day trends during different seasons for all the districts of Haryana, India by using the mean rainfall, rainfall deviation, seasonal rainfall ratio (SRR), coefficient of variation (CV), number of rain days, rainfall intensity, trends of rain days, empirical orthogonal functions (EOF) and Principal Component (PC) analysis [7].

Chinese scholars have also carried out related research. Gu took the cases of the annual maximum peak flows at 28 stations across the Pearl River basin by using two nonparametric (Mann-Kendall and Spearman) tests to detect the temporal trends. Generalized additive models for location, scale and shape (GAMLSS) and long-term persistence are used to test the stationarity assumption [8]. Yin chose the precipitation data of 14 meteorological stations in the Poyang Lake Basin to model the changes of extreme precipitation from 1951 to 2010 based on both stationary and non-stationary Generalized Extreme Value (GEV) models [9]. In order to explore the temporal and spatial variation of extreme precipitation and its non-stationary characteristics, the GAMLESS model was used to detect the temporal and spatial variation characteristics of extreme precipitation [10]. Kong analyzed the Spatio-temporal pattern of the precipitation concentration degree (PCD) and precipitation concentration period (PCP) in China. The results showed that PCD and PCP were decreasing in China as a whole [11]. Wang studied the non-uniform characteristics of precipitation concentration in Jiangsu Province, and found that it showed a decreasing trend for many years. The precipitation in the north was more concentrated than in the south [12]. Wang found that both PCD and PCP were increasing in the southeast coastal areas of China [13]. Li analyzed the characteristics of precipitation concentration in 1960 and 2014 in the north and south of Qinling Mountains and considered that the precipitation concentration degree in the south of Qinling Mountains was higher than that in the north of Qinling Mountains, and the precipitation concentration degree in Qinling Mountains showed a significant upward trend [14]. At the level of analyzing the characteristics of precipitation concentration in the basin, Zhou discussed the characteristics of daily precipitation concentration in the Huaihe River Basin from 1951 to 2009 [15]. Huang analyzed

the change trend of daily rainfall concentration and rainfall statistical characteristics in the middle and upper reaches of Wujiang River Basin [16]. The studies found that the daily precipitation concentration degree of each station showed an increasing trend, and the correlation between the daily precipitation concentration degree and maximum daily rainfall was high. Using the defined annual precipitation concentration degree and period concentration index, Pang found that the annual precipitation distribution in the Huaihe River Basin was uneven and the precipitation season was more concentrated [17]. The variation trend of the monthly and seasonal precipitation concentration index aggravates the polarization of precipitation distribution, showing the temporal variation characteristics of "drier the drier, wetter". Li discussed the variation characteristics of precipitation concentration in the flood season and mid-period in the Xianhe River Basin in the upper reaches of Huaihe River [18]. The analysis of precipitation characteristics was also widely used in the Hanjiang River Basin [19], Lancang River Basin [20], Luanhe River Basin [21], Southwest region and Loess Plateau [22,23]. At the same time, scholars also pay attention to the correlation between PCD, PCP and annual precipitation. The results showed that there was a good correlation between PCD and annual precipitation, while the correlation between PCP and precipitation was poor. The results also revealed the relationship between precipitation, PCD, PCP and the occurrence and development of drought and flood [24]. Despite the fact that the temporal analysis of precipitation is straightforward, the spatial analysis is more complex. Due to the influence of land and sea position, latitude location and topography, the spatial distribution of precipitation is uneven. The influence of the summer monsoon is the main reason for the uneven temporal and spatial distribution of precipitation in China. The eastern coastal monsoon area is obviously affected by the summer monsoon, while the non-monsoon area is restricted by land and sea location.

The Wujiang River Basin is the largest tributary on the south bank of the upper reaches of the Yangtze River in China. It is a typical mountain small river basin with numerous tributaries and a feathery water system distribution. The Wujiang River basin runs through the west, central and northeast of Guizhou and the east of Chongqing, and is high in the west and low in the east. The special topography and geographical features of the mountain area have created unique climate characteristics in the basin [25]. Analyzing and understanding the climatic and weather characteristics of precipitation in Wujiang River Basin is of practical significance to improve the ability of precipitation climate prediction and weather forecast [26,27]. According to the analysis of the characteristics of precipitation concentration in Wujiang River basin, research on the monthly scale and daily scale has been carried out. But the research on ten-day scale has not been fully carried out and the time series of existing research on precipitation concentration needs to be updated. Therefore, based on the ten-day scale, this paper uses the precipitation concentration degree and mid-concentration method to analyze the variation characteristics of the precipitation concentration degree (PCD) and rainfall concentration period (PCP) in Wujiang River Basin from 1963 to 2021. Here, the characteristics of non-uniformity of precipitation distribution are studied by using the Randall S analysis method, Mann–Kendall test method, Pettitt method, wavelet analysis and empirical orthogonal function (EOF). The research results are expected to provide a reference for the utilization of water resources, flood-control planning and flood-disaster-emergency planning in the Wujiang River basin, and provide a basis for meteorological scientific disaster prevention and reduction.

2. Materials and Methods

2.1. Materials

The geographic information data of Wujiang River basin was derived from geospatial data cloud DEM digital-elevation data with a spatial resolution of 30 m and a data type of IMG. Figure 1 shows the topographic map of Wujiang River basin drawn by ArcGIS. The meteorological data came from the Meteorological Information Center of China Meteorological Administration, mainly based on daily precipitation data. The starting and ending time of the data was from 1 January 1963 to 31 December 2021. Its scope included

12 regions in Guizhou, Yunnan, Sichuan and Hubei provinces. A total of 40 meteorological stations in the basin were selected for analysis. The information statistics of Wujiang River Basin stations are shown in Table 1. The missing test data were supplemented by linear interpolation. The average daily precipitation data of 40 meteorological stations were used as the daily precipitation series of the whole Wujiang River basin to calculate the PCD and PCP values and related indexes of the whole basin. The stations outside the watershed were only used for spatial difference analysis.
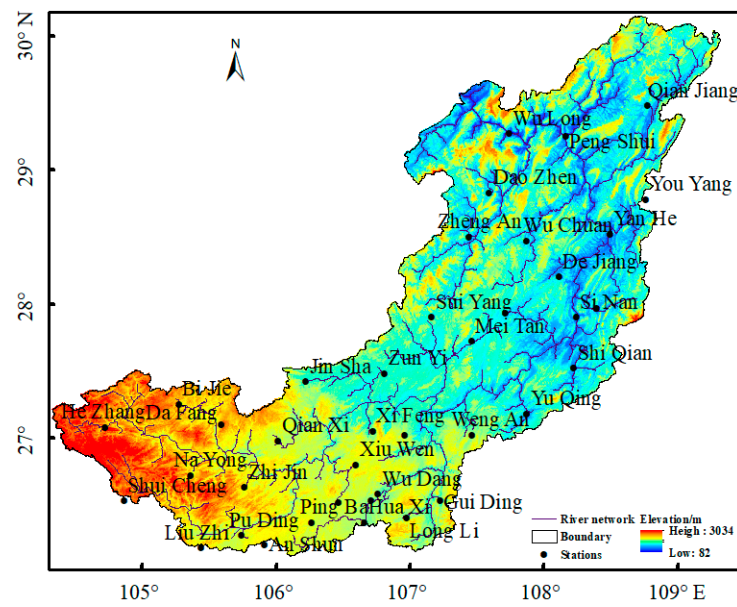

Figure 1. Topography distribution in Wujiang River basin.

Table 1. Wujiang river basin weather station statistics.

Station	Altitude (m)	MAP [1] (mm)	Station	Altitude (m)	MAP (mm)
HZ	1535.1	844.1	WA	1129.6	1111.6
WN	2237.5	900.4	YQ	622.1	1076.4
SC	1815.9	1187.4	SN	416.8	1125.2
WL	406.9	1045.7	YJ	521.5	1109.4
QJ	786.9	1186.3	SQ	467.5	1111.1
PS	322.2	1227.3	NY	1457.1	961.1
DZ	685.6	1053.9	QX	1231.4	1386.2
ZA	816.4	1066.8	ZJ	1319.3	1309.5
YY	826.5	1343.8	AS	1431.1	1467.8
WC	660.3	1209.3	LZ	1361.9	1342.4
YH	334.6	1146.5	PD	1274.5	961.1
DJ	629.5	1215.6	XW	1296.7	1140.6
BJ	1510.6	891.8	QZ	1300	1171.4
DF	1700	1052.1	PB	1298.2	1271.1
ZY	843.9	1035.1	GY	1223.8	1113.5
JS	942	1026.3	GD	925	1154.9
XF	1112.1	1193.9	FG	710.2	1052.1
KY	1275.6	1119.5	LL	1093.7	1089.9
SY	889.3	1117.5	HX	1149	1138.1
MT	792.2	1211.7	WD	1104	1140.6

[1] Average annual precipitation.

2.2. Methods

2.2.1. Precipitation Concentration (PCD) and Mid-Concentration (PCP)

The main parameters characterizing the time distribution of precipitation at a single station were the precipitation concentration (PCD) and mid-concentration (PCP) in this study. Its calculation formula is as follows:

$$PCD_i = \sqrt{(\sum_{j=1}^{N} r_{ij} \times \sin\theta)^2 + (\sum_{j=1}^{N} r_{ij} \times \cos\theta)^2 \,/R_i} \tag{1}$$

$$PCP_i = \arctan(\sum_{j=1}^{N} r_{ij} \times \sin\theta_j / \sum_{j=1}^{N} r_{ij} \times \cos\theta_j) \tag{2}$$

In the formula: i is the year (i = 1963, 1964, ..., 2021), j is the ten-day period of the year (i = 1, 2, ..., 36), N is the total year, r_{ij} is the j ten-day precipitation (mm) of the i year, R_i is the i-year annual precipitation (mm) of a certain station, θ_j is the vector angle corresponding to each ten days in the study period, θ_j = 360° $\times$ ($j - 1$)/36. PCD_i and PCP_i are i-year precipitation concentration (dimensionless) and mid-day (ten-day), respectively. And the value of PCD_i is between 0 and 1, which reflects the concentration of annual precipitation in each ten-day period. The closer PCD_i is to 1, it indicates that the annual precipitation is concentrated in a certain ten-day, and the closer PCD_i is to 0 indicates that the precipitation is evenly distributed in each ten-day period of the whole year. PCP_i is the azimuth of the composite vector, which reflects the ten-day period in which the maximum ten-day precipitation occurs.

2.2.2. R/S Analysis

R/S analysis, also known as rescaled range analysis (Rescaled Range Analysis), is usually used to analyze the fractal characteristics and long-term memory process of time series. It is a method put forward by hydrologist Hurst on the basis of a large number of empirical studies, and then gradually improved through the efforts of many people. In this method, the Hurst index is calculated by using the time series of climatic elements to reveal the trend of the time series of climatic elements.

For a time series $x(t)$, t = 1, 2, ..., the mean series is as follows:

$$y(f) = \frac{1}{f}\sum_{t=1}^{f} x(t) \quad f = 1, 2, 3 \cdots \tag{3}$$

The cumulative deviation is as follows:

$$X_0 = [x_0(1), x_0(2), \cdots, x_0(t)], \; X_i = [x_i(1), x_i(2), \cdots, x_i(t)] \; i = 1, 2, \cdots, nk \tag{4}$$

The range is as follows:

$$R(f) = \max_{1 \le t \le f} F(t, f) - \min_{1 \le t \le f} F(t, f) \quad F(t, f) = 1, 2, \cdots \tag{5}$$

The standard deviation is as follows:

$$S(f) = [\frac{1}{f}\sum_{t=1}^{f} (x(t) - y(f))^2]^{1/2} \quad f = 1, 2, \cdots \tag{6}$$

Finally, by R/S analysis, it is found that there is a certain relationship between $R(f)$ and $S(f)$, which is as follows:

$$R(f)/S(f) = C(f)^H \tag{7}$$

where C is the proportional coefficient and H is the Hearst index. For different H, it means different trend changes: when $0.5 < H < 1.0$, it indicates that the long-term correlation characteristic of time series is persistence, and the closer the Hurst index value is, the stronger the persistence is. When $0.0 < H < 0.5$, the long-term correlation characteristic of time series is anti-persistence, and the closer the Hurst value is, the stronger the anti-persistence is. The important application value of R/S analysis is to use the trend component of Hurst index to predict the future climate change trend.

2.2.3. Nonparametric Statistical Test Method

Mann–Kendall test method is a commonly used non-parametric statistical test method. Variables, which is more suitable for type variables and sequential variables, cannot have the characteristics of normal distribution and also not be disturbed by a small number of outliers. For the time series x with the number of samples n, the order sequence is constructed as follows:

$$S_k = \sum_{i=1}^{k} r_i \quad (k = 2, 3, \cdots, n) \tag{8}$$

The value of r_i in the formula is as follows:

$$r_i = \begin{cases} +1 & x_i > x_j \\ +0 & x_i \le x_j \end{cases} \quad j = 1, 2, \cdots, i \tag{9}$$

It can be seen that the order column S is the cumulative count of the number of values at the first time greater than the number at the time j. Statistics are defined under the assumption that the time series are random and independent. The Z value is used to detect a statistically significant trend.

$$Z = UF_k = \frac{[s_k - E(s_k)]}{\sqrt{\text{var}(s_k)}}, \quad k = 1, 2, \cdots, n \tag{10}$$

In Equation (10): $UF_1 = 0$, $E(S_k)$ and $var(S_k)$ are the mean and variance of S_k. When x_1, x_2, ..., x_n is independent of each other and has the same continuous distribution, they can be calculated from the following formula:

$$\begin{cases} E(s_k) = \frac{k(k-1)}{4} \\ \text{var}(s_k) = \frac{k(k-1)(2k+5)}{72} \end{cases} \quad k = 2, 3, \cdots, n \tag{11}$$

UF_k is a standard normal distribution, which is a series of statistics calculated according to the time series order x_1, x_2, ..., x_n and then reverse x_n, x_{n-1}, ..., x_1 according to the time series. Then, repeat the above process and make $UB_k = -UF_k$, $k = n$, $n - 1$, ..., 1. $UB_1 = 0$. UF_k reflects the overall changing trend of the sequence. When $UF_k > 0$, the sequence shows an overall upward trend, and when $UF_k > 1.96$, the upward trend reaches significant levels (0.05). When $UF_k < 0$, the sequence showed a downward trend, and when $UF_k < -1.96$, the downward trend reached significant levels (0.05). Sen's slope was also applied to evaluate the linear trend slope. In particular, the slope showed in Equation (12) is the median of β computed for each year y:

$$\beta = median((x_{jy} - x_{ky})/(j - k)) \quad \forall k < j \ y = 1, 2, \ldots, N \tag{12}$$

Overall, the positive and negative Sen's slope β values may indicate the potential presence of increasing and decreasing trends, respectively. In this context, Sen's slope provides the average increase or decrease for precipitation, PCD and PCP on an annual scale.

The Mann–Kendall method can identify the time when the mutation begins and point out the mutation region, but it is not suitable for detecting sequences with multiple mutation

points. The Pettitt method, like that of Mann–Kendall, constructs an order sequence like Equation (1), except that r_i is defined in three cases and showed as follows:

$$r_i = \begin{cases} +1 & x_i > x_j \\ 0 & x_i = x_j \ \ j = 1, 2, \cdots, i \\ -1 & x_i < x_j \end{cases} \tag{13}$$

The Pettitt method directly uses the order series to detect the mutation points, which can better identify the time series mutation points and judge whether the mutation points are statistically significant. If t_0 is satisfied at all times, the k is defined as follows:

$$k_{t_o} = Max|S_k| \ \ (k = 2, 3, \cdots, n) \tag{14}$$

Then, t_0 is the point of sudden change P, which is defined as follows:

$$P = 2\exp[-6k_{t_0}{}^2(n^3 + n^2)] \tag{15}$$

If $P < 0.5$, it is considered that the detected mutation point is statistically significant.

2.2.4. Wavelet Analysis

The advantage of wavelet analysis is that it can accurately extract information from time-frequency local transform signals. Therefore, wavelet analysis is widely used in the field of climate research to analyze the climate data of time series and identify the transformation characteristics and periodicity of climate factors at different time scales. At the same time, the wavelet variance image obtained by wavelet coefficients can directly show the main period of climatic factors changing with time.

Define wavelet function $\int_{-\infty}^{+\infty} \psi(t)dt = 0$. $\psi(t)$ forms a cluster of functions by stretching and translating:

$$\psi_{a,b}(t) = |a|^{-\frac{1}{2}}\psi(\frac{t-b}{a}) \ \ b \in R, a \in R, a \neq 0 \tag{16}$$

In Equation (16), $\psi_{a,b}(t)$ is the sub-wavelet; a is the scale factor, which reflects the period length of the wavelet; and b is the time factor, which reflects the translation in time. For the time series $f(t) \in L^2(R)$, the associated wavelet transform is defined as follows:

$$W_f(a, b) = |a|^{-\frac{1}{2}}\int_{-\infty}^{+\infty} f(t)\overline{\psi}(\frac{t-b}{a})dt \tag{17}$$

In Equation (17), $\psi(t)$ is the complex conjugate function of $\psi(t)$, and $W_f(a,b)$ is the wavelet coefficient. The square of all wavelet coefficients with respect to a in the time domain is integrated, that is, the wavelet variance: $Var(a) = \int_{-\infty}^{+\infty}\left|W_f(a,b)\right|^2 db$. The variation process of wavelet variance with scale a is called the wavelet variance map, which reflects the distribution of wave energy with scale and can be used to determine the main time scale (main period) in a time series.

With the change in parameters a and b, we can make a two-dimensional Isoline map with $W_f(a,b)$ as Abscissa and an as ordinate. The wavelet features about the changes of time series can be obtained from the graph. The wavelet coefficients at different time scales can reflect the variation characteristics of the system at this time scale. Through the analysis of wavelet coefficients, the multi-time scale periodicity and abrupt change in annual rainfall and runoff time series can be identified.

In this study, in the MATLAB2018b software, the wavelet toolbox in wavelet analysis was used to process the temperature and precipitation series data. The Morlet negative wavelet function was used to process the extended data series. C_{mor} was selected as the wavelet function type to analyze the multi-time scale characteristics of air temperature and precipitation.

3. Temporal Variation Characteristics of Precipitation in Wujiang River Basin

3.1. Trends of PCD and PCP

Figure 2a,b shows the variation characteristics of *PCD* and *PCP* respectively in the Wujiang River Basin. The fluctuation range of *PCD* in the Wujiang River Basin from 1963 to 2021 was 0.34–0.59, with an annual average of 0.47, which is significantly higher than the national average (0.15–0.25), indicating that the annual precipitation distribution in the whole basin is relatively concentrated. From the comparison of the watershed, it was also higher than the Huaihe River basin in the south (0.35–0.61) and almost the same as the Songhua River basin in the north (0.682). The maximum value appeared in 1999 and the minimum value appeared in 2006, and the precipitation distribution was relatively uniform and the difference was small. The *PCD* in Wujiang River Basin showed an increasing trend from 1963 to 2021 and the tendency rate was 0.003/(10a), which indicate that the precipitation will tend to be concentrated in the future.


(a)　　　　　　　　　　　　　　　　　(b)
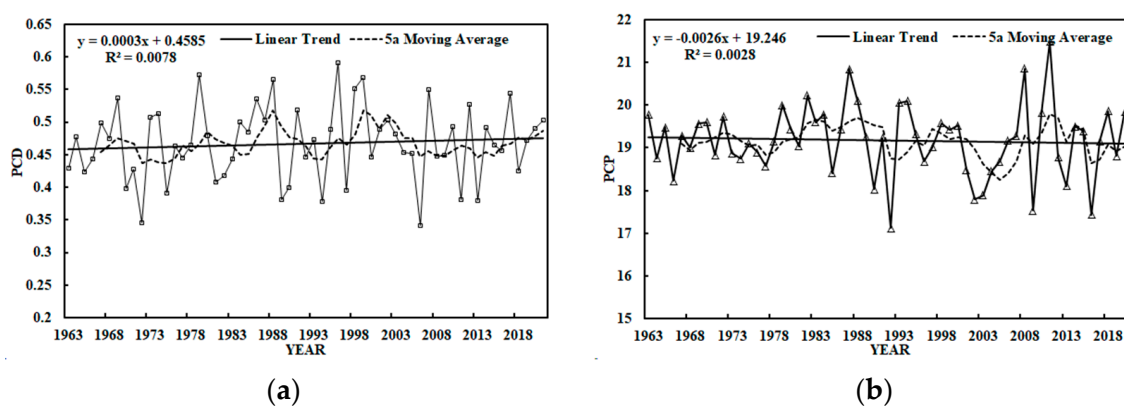
Figure 2. Dynamic changes of precipitation concentration PCD (**a**) and PCP (**b**) in Wujiang River Basin from 1963 to 2021.

The fluctuation range of *PCP* from 1963 to 2021 was between 17.1 and 21.5 days, that is, the middle period of multi-year average precipitation occured from mid-June to late July. The earliest was in mid-June 1992, the latest in late-July 2011, and the multi-year average was 19.2 days, that is, from the first ten days of July to the middle of July. The *PCP* in Wujiang River basin shows a weak decreasing trend, and the tendency rate is −0.026/(10a), which indicate that there is an early trend of precipitation concentration in the middle period.

3.2. Analysis of Mutation Characteristics of PCD and PCP

The Mann–Kendall test method was used to analyze the time-variation characteristics of precipitation concentration in the Wujiang River basin. From Figure 3a,b, it can be found that the *UF* statistics of *PCD* were positive, except for negative values in 1965 and 1972. *PCD* showed a slow increasing trend and *UF* statistics increased rapidly from the lowest value in 1972 to the highest value in 1988, which indicate that *PCD* increased significantly during this period and then tended to be stable. The *UF* statistics of *PCP* increased rapidly from the lowest value in 1972 to the highest value in 1988, which indicates that *PCP* increased significantly during this period and then fluctuated downwards to stabilize after 2008. There are multiple intersection points between *UF* and *UB* statistics of PCD and PCP. The intersection points were all in the confidence interval, which indicates that there were multiple mutation points in PCP and PCD.

(a)

(b)

(c)

(d)
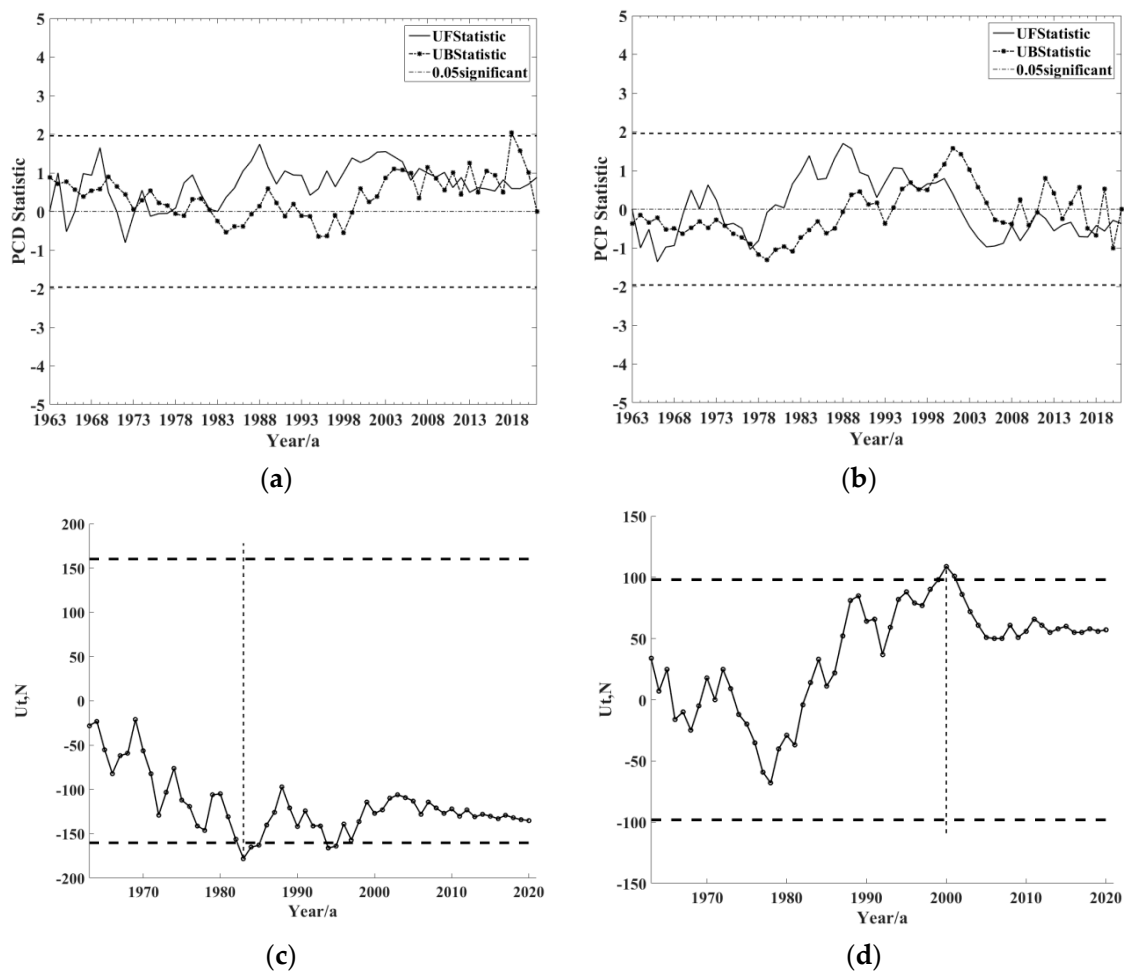
Figure 3. Abrupt change test of time series of precipitation concentration degree PCD (**a**,**c**) and PCP (**b**,**d**) in Wujiang River Basin.

The value of parameters Z, β and P for annual precipitation, PCD and PCP are presented in Table 2. These *p* values can be used to assess which clusters exhibit significant trends or not. The MK test for annual precipitation and PCP revealed negative values of both Z and β, which shows decreasing trends in clusters precipitation (Z = −1.996, β = −106.33%) and PCP (Z = −0.732, β = −0.23%). On the contrary, PCD revealed positive values of both Z and β, which shows increasing trends in cluster PCD (Z = 1.753, β = 0.03%). It must be pointed out that, although significant differences were observed among PCD and PCP, no *p*-values below 0.05 were found, with *p* ranging from 0.080 (precipitation) to 0.464 (PCP). This means that there are no statistically significant trends.

Table 2. Parameter value Mann–Kendall test.

Types	Mean Value	Z	*p*	β (%)	L$_β$ (%)	U$_β$ (%)
precipitation	1140.94	−1.996	0.046	−106.33	−363.40	93.08
PCD	0.47	1.753	0.080	0.03	−0.06	0.13
PCP	19.17	−0.732	0.464	−0.23	−1.42	1.04

The Pettitt method is used to detect the precipitation concentration and the abrupt change point in the middle stage of precipitation concentration in Wujiang River Basin. Figure 3c shows the results of *PCP* test using the Pettitt method. The statistic $U_{t,N}$ showed the lowest value of −178 in 1983, which exceeded the critical threshold of 0.05 significance level −160.2, indicating that *PCD* in Wujiang River basin had a significant mutation before

and after 1983. From 1963 to 1983, *PCD* showed an obvious downward trend, and its average value was 0.46 million from 1984 to 2021, and the average value was 0.47. According to the test results of *PCP* (Figure 3d), the maximum statistic $U_{t,N}$ that appeared in 2001 was 109, which exceeded the critical threshold of the 0.05 significance level. The result showed that there was a significant mutation of *PCP* in Wujiang River Basin before and after 2001. The value of parameter P for PCD and PCP were 0.80 and 0.85, respectively. It is believed that the detected mutation points are not statistically significant.

3.3. Periodic Variation Characteristics of PCD and PCP

The real part equivalent map of wavelet coefficients can reflect the periodic variation of the precipitation series at different time scales and its distribution in the time domain, and then judge the future variation trend of precipitation on different time scales. The magnitude of the central value can reflect the oscillation intensity of the fluctuation. A positive value of *PCD* means "tends to concentrate", a negative value means "tends to disperse", a positive value of *PCP* "tends to postpone", and the negative value means "tends to advance". The wavelet variance map shows the distribution of periodic fluctuation energy of precipitation time series on the time scale. The modulus of the wavelet coefficient represents the energy density. The larger the modulus is, the more obvious the periodicity of the corresponding period and scale is. The modulus square of wavelet coefficients is equivalent to the wavelet energy spectrum, and the oscillation energy of different periods can be analyzed from the modulus square map of wavelet coefficients.

Figure 4a shows the periodic variation characteristics of *PCD*. It can be seen that *PCD* had periodic changes of about 40 years, 10 years and 5 years, and the periods of about 40 years were global, showing the changing characteristics of "dispersion-concentration-dispersion". The period of about 10 years oscillated obviously after 1985, and the periodic oscillation of about 5 years mainly existed before 2000. It can be seen from Figure 4b that the wavelet variance of *PCD* was the maximum at 40 years, which was the first main period, indicating that the precipitation in Wujiang River basin will undergo a change process from relatively concentrated to more uniform in about 40 years. After 2010, the precipitation concentration will be enhanced, and the positive closed center will not be formed, indicating that the precipitation concentration will continue to increase in the future. Figure 4c shows the periodic variation of *PCP*. It can be seen from Figure 4c that there are periodic changes of about 35 years, 15 years and 5 years in *PCP*, and the cycle of about 35 years is global. The result shows that there are two periodic changes of advance postponement. It can be seen from Figure 4d that the wavelet variance of *PCP* has a peak at the scale of 40 years, which indicates that the main period of *PCP* is about 40 years, that is, the maximum precipitation of Wujiang River basin will go through a change process from late to early in about 40 years. After 2015, the precipitation will enter the late period and will not form a closed center, and the maximum precipitation in flood season of Wujiang River will continue to be delayed.

At present, it is considered that there is an obvious correlation between the periodic variation of hydrological series, the short wave in the motion law of celestial bodies, and the intensity of sunspot activity. The weather variation process of the 35-year cycle is the Bruckner cycle, the 11-year cycle is the sunspot cycle, and the 5–6-year cycle is the solar double-vibration cycle, which is all caused by solar activity. Therefore, it can be considered that the periodic variation of precipitation in the Wujiang River basin is closely related to the motion of celestial bodies.
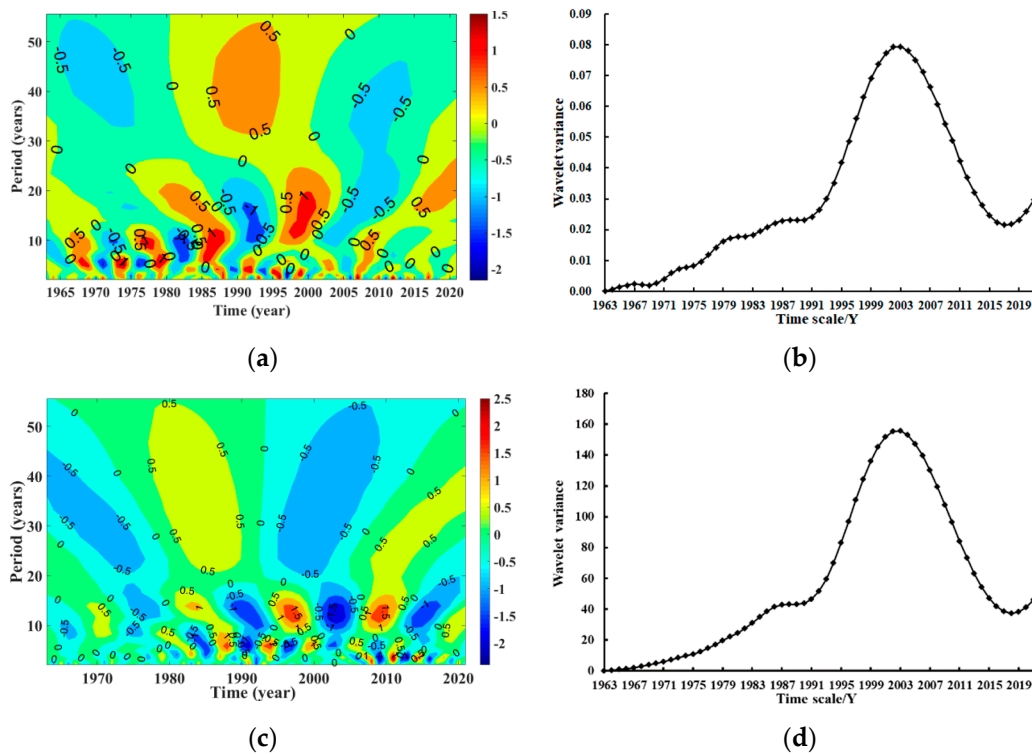
Figure 4. PCD and PCP wavelet analysis of Wujiang River Basin from 1963 to 2021 ((**a**,**c**) real equivalent map; and (**b**,**d**) wavelet variance).

3.4. Forecast of Changing Trend of PCD and PCP

The change trend of future *PCD* and *PCP* in Wujiang River Basin was analyzed by the R-Randall *S* analysis method. The Hurst index and change trend of *PCD* and *PCP* in Wujiang River Basin are shown in Figure 5. The fitting coefficients of *PCD* and *PCP* in Wujiang River Basin were 0.9587 and 0.9442, respectively, and the fitting effect was significant. The Hurst index of *PCD* was 0.53, which indicates that the projected *PCD* in Wujiang River Basin is consistent with the change trend in the past 60 years. At the same time, the Hurst index was close to the critical value of 0.5, which indicates that the periodic law may be implied in the study area. The *Hurst* index of *PCP* was 0.6, which indicates that there is an obvious Hearst phenomenon in *PCP*. The projected change trend is consistent with that of the past 60 years, that is, the precipitation concentration period will remain in advance.
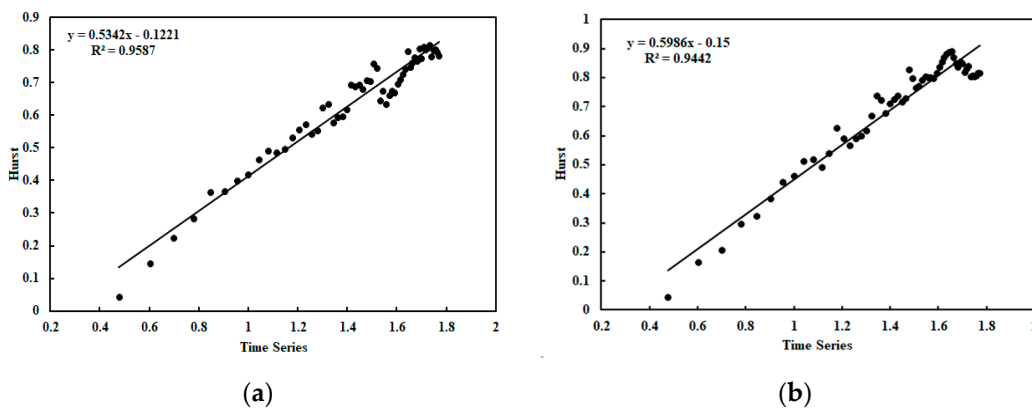
Figure 5. Distribution of precipitation concentration PCD (**a**) and mid-concentration PCP (**b**) in Wujiang River Basin.

4. Spatial Distribution Characteristics of PCD and PCP in Wujiang River Basin

4.1. Characteristics of Multi-Year Average Spatial Distribution

Figure 6 shows the spatial distribution characteristics of PCD and PCP in the Wujiang River Basin. The multi-year average PCD of each station in the Wujiang River Basin from 1963 to 2021 was 0.39–0.60. The overall precipitation concentration is uniform and shows a trend of gradually increasing from the downstream to the upstream, which indicate that the precipitation concentration in the upper reaches is high and more concentrated. The maximum value is above 0.56, which appears in Hezhang, Weining, Liuzhi and Puding stations in the upstream. The precipitation concentration in the upper reaches of the Wujiang River basin is higher than that in the upper reaches. Among them, the PCD of Hezhang Station is more than 0.6. The precipitation in the middle reaches and downstream is relatively low and the minimum is in Kaiyang and Weng'an in the middle reaches and Youyang in the lower reaches. The PCD is about 0.41 and less than 0.4 in Kaiyang. The multi-year average value of PCP in each station of Wujiang River is 14.6~22.1. The spatial distribution shows an obvious distribution pattern of high and low values, which increases gradually from southeast to northwest. In most upstream areas, the PCP value was about 19~22 (that is, July and early August) and the maximum value was 22.1 in Huaxi. The PCP value in the southeast of the lower reaches was 14~16 (mid-May and early June), and the minimum value was 14.4 in Yinjiang River. The PCP value of other parts of the basin was about 17~18 (that is, mid-June and late-June). Generally speaking, the precipitation in the southeast of the upper reaches of the Wujiang River Basin is mainly concentrated in mid–early July, while the precipitation in the middle-lower reaches is mainly concentrated in late June and early July.
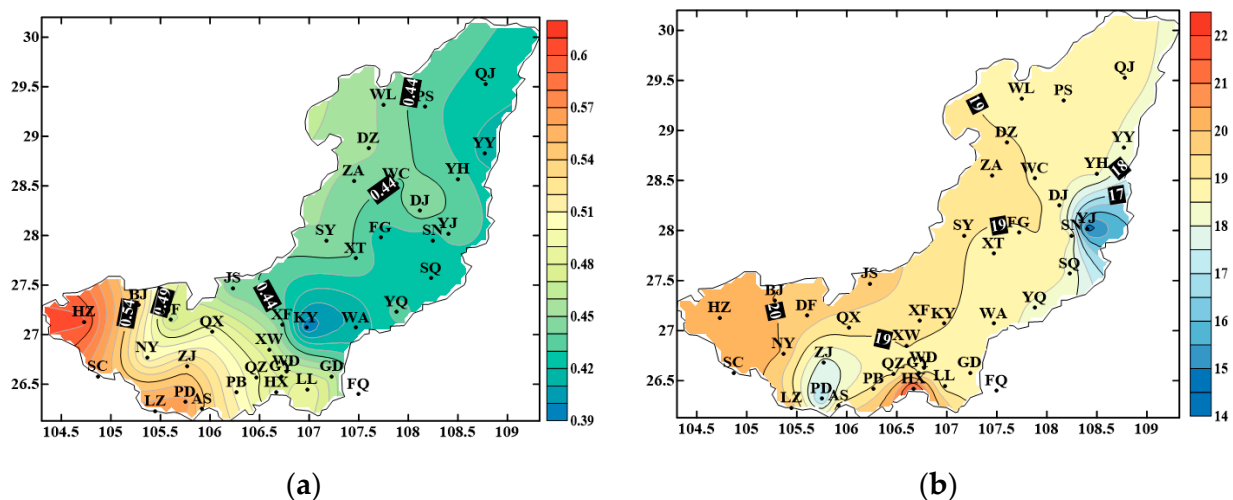

Figure 6. Spatial distribution of precipitation concentration PCD (**a**) and PCP (**b**) in Wujiang River Basin.

4.2. Main Spatial Distribution Patterns of PCD and PCP

Empirical orthogonal decomposition (EOF) was used to reveal the main spatial distribution characteristics of PCD and PCP anomalies in Wujiang River Basin, based on the normalized anomaly data of meteorological stations from 1963 to 2021. Only the first two modes passed the north test. The variance contribution rate of the first mode of PCD was 73.6%. Its spatial distribution characteristics are shown in Figure 7a. It can be seen that the overall eigenvalues of the middle–lower reaches of the basin are positive and the characteristic values of the upper reaches of the basin are negative. The results indicate that the spatial change in PCD shows an opposite pattern between the upper reaches of the basin and the middle–lower reaches of the basin, that is, the more concentrated (non-concentrated) precipitation is in the upper reaches of the southwest, and the less concentrated (concentrated) is in the middle–lower reaches of the northeast. The high-value

center of this mode is located in the south of the middle reaches of the basin, which indicates that the variation of precipitation concentration in these areas is more significant. Figure 7b shows the spatial distribution of the second mode of PCD. The variance contribution rate of this mode was 7.8%, and its spatial pattern shows the opposite pattern between the upper reaches and the lower reaches of the basin. That is, the more concentrated (not concentrated) the precipitation in the upstream area, the less concentrated (concentrated) the precipitation in the downstream area. The high-value center of this mode is located in the north of the lower reaches of the basin. Compared with the upstream and downstream, the change in precipitation concentration in the middle reaches is not obvious.
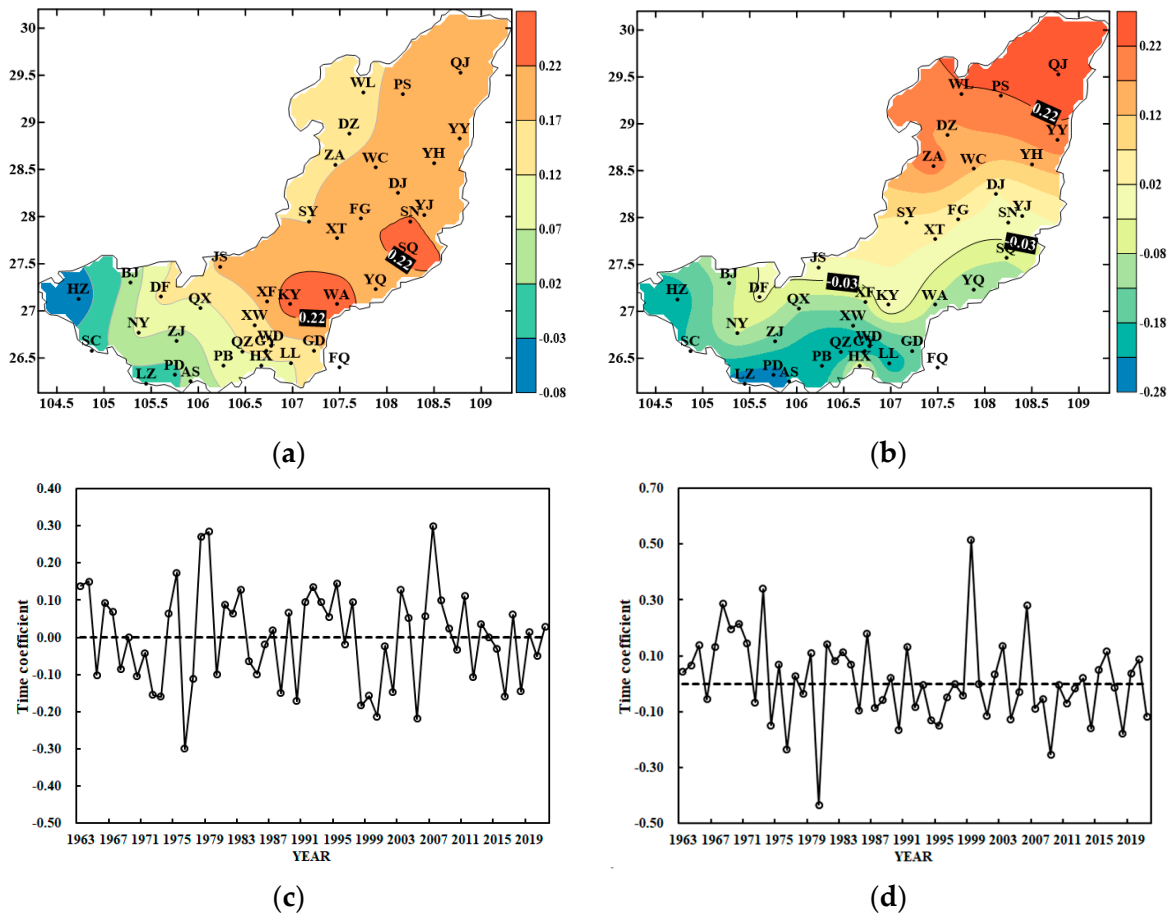
Figure 7. Spatial distribution of first mode (**a**), second mode (**b**), time series of first mode (**c**) and time series of second mode (**d**) of EOF decomposition of PCD in Wujiang River Basin.

Figure 8a is the spatial distribution of the first mode of PCP, and the variance contribution rate of this mode was 50.1%. Similar to PCD, the spatial variation of PCP in Wujiang basin also showed the opposite pattern between the upper reaches of the basin and the middle–lower reaches of the basin. The high-value center is located in the middle-lower reaches of the Yinjiang River, indicating that the mid-term changes of precipitation in these areas are obvious. Figure 8b shows the spatial distribution of the second mode of PCP; the contribution rate of variance was 19.6%. Different from the second mode pattern of PCP, the eigenvalues of other areas are positive, except the eigenvalues of the southern part of the upper reaches of the Wujiang River basin and the Yinjiang region of the middle–lower reaches, which are negative. On the whole, it shows consistency in space.
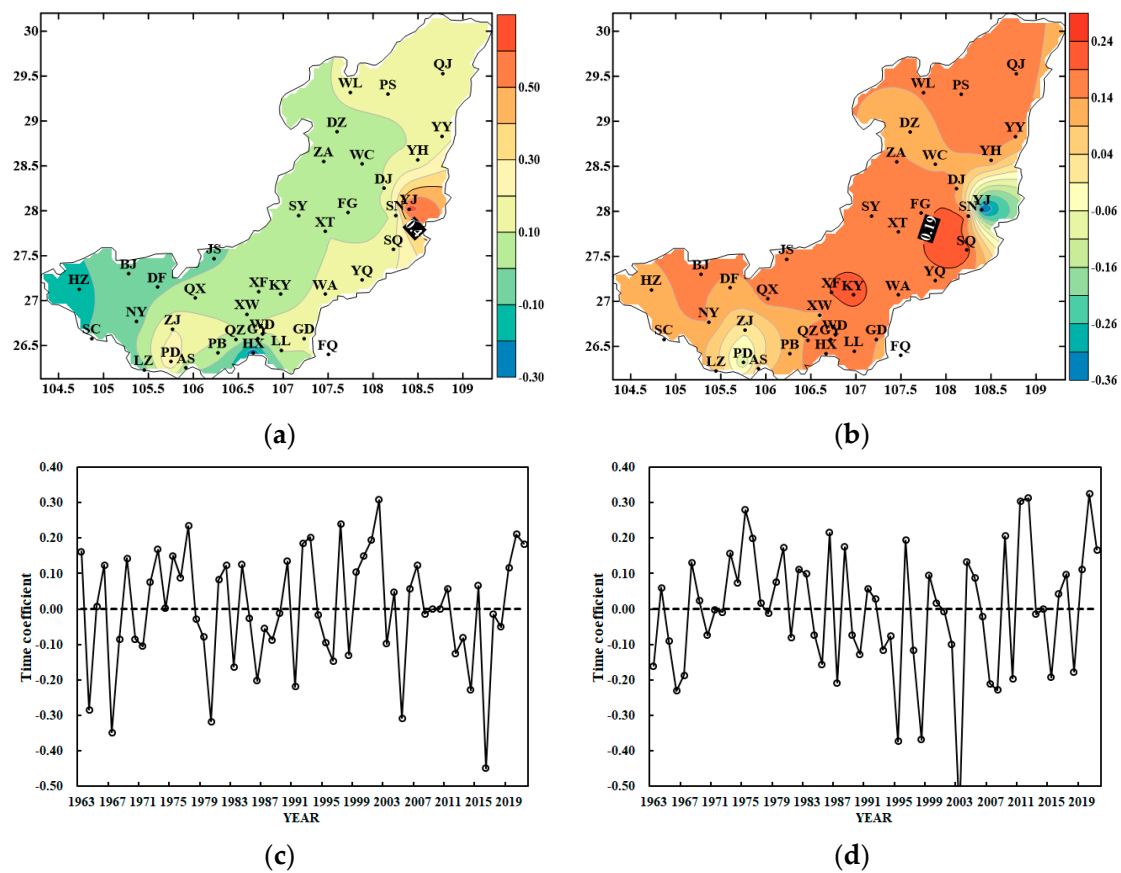
Figure 8. Spatial distribution of first mode (**a**), second mode (**b**), time series of first mode (**c**) and time series of second mode (**d**) of EOF decomposition of PCP in Wujiang River Basin.

The above research results show that the spatial pattern of the first mode of PCD and PCP in the Wujiang River basin from 1963 to 2021 is consistent, showing an opposite pattern between the upper reaches and the middle–lower reaches of the basin. It reflects the influence of watershed topography on the spatial distribution of precipitation. The most obvious influence of topography on precipitation in the upper reaches of the basin is the mountain range in the south. Precipitation is blocked by topography, resulting in topographic rain, and topographic rain forms a rapidly changing rain belt. The influence of mountains on topography is mainly highlighted by the "topographic rain" of windward slope and the "wind incineration effect" of leeward slope. The topography in the middle reaches of the basin is relatively flat, and the spatial variation of precipitation is gentle. The influence of topography on precipitation is smooth in space. The terrain in the lower reaches of the basin is undulating, with mountains in the northeast-southwest direction. The effect of altitude on precipitation is also in the northeast–southwest direction. However, due to the relatively low altitude, the influence of topography on precipitation is limited. The spatial difference of precipitation pattern in the upper reaches of the basin and the middle–lower reaches of the basin leads to the opposite change trend of PCD and PCP in the corresponding space.

5. Conclusions and Prospect

Based on the daily precipitation observation data of 40 meteorological stations in Wujiang River Basin from 1963 to 2021, the temporal and spatial variation characteristics of the precipitation concentration degree (PCD) and precipitation concentration metaphase (PCP) were analyzed using Randall S analysis, the Mann–Kendall test, the Pettitt method, wavelet analysis and empirical orthogonal decomposition (EOF). The main results are as follows:

(1)　The fluctuation range of PCD in Wujiang River Basin from 1963 to 2021 was 0.34–0.59, with an annual average of 0.47, which was significantly higher than that of the whole country. The fluctuation of PCD shows a slowly increasing trend, indicating that the precipitation will tend to be concentrated in the future. The fluctuation range of PCP is from 17.1 to 21.5 days, with a multi-year average of 19.0. Most of the precipitation in the year is concentrated around the middle of July, showing a slowly decreasing trend, indicating that there is an early trend in the middle period of precipitation concentration in the future. There was a significant mutation in PCD around 1983 and a significant mutation in PCP around 2001.

(2)　The precipitation in Wujiang River Basin will experience a change process from more concentrated to more uniform in about 40 years, and the degree of precipitation concentration will continue to increase in the future. The maximum precipitation in the Wujiang River Basin will experience a change process from late to early in about 40 years, and the maximum precipitation in the future will continue to be delayed. The Hurst index of PCD is 0.53, which is close to the critical value of 0.5, indicating that the periodic law may be implied in the study area. The Hurst index of PCP is 0.6, which indicates that there is an obvious Hearst phenomenon in PCP; that is, the precipitation concentration period will keep ahead of time.

(3)　The overall precipitation concentration degree (PCD) in the Wujiang River Basin is relatively uniform, showing a gradual increase from the downstream to the upstream, indicating a higher concentration of precipitation in the upstream areas. The concentration period of precipitation is lower in most areas of the middle and lower reaches. The multi-year average of PCP (precipitation) at various stations in the Wujiang River Basin ranges from 14.6 to 22.1, with a spatial distribution pattern characterized by distinct high and low values, gradually increasing from southeast to northwest. Overall, precipitation in the southeastern part of the upstream region of the Wujiang River Basin is mainly concentrated in the first half of July, while precipitation in the middle and lower reaches is mainly concentrated in late June and early July.

(4)　The spatial variation of the precipitation concentration degree (PCD) in the Wujiang River Basin exhibits an opposite pattern between the upstream and downstream regions. In the upstream areas, precipitation becomes more concentrated (less dispersed), while in the downstream areas, precipitation becomes less concentrated (more dispersed). The high-value center of this pattern is located in the northern part of the downstream region. Compared to the upstream and downstream, the middle reaches show less-noticeable changes in precipitation concentration. The spatial variation of the PCP (precipitation) also demonstrates a similar contrasting pattern between the upstream and middle–lower reaches of the basin, with the high-value center located in the middle–lower reaches, particularly in the Yinjiang area. This indicates a more-pronounced variation in the concentration period of precipitation in these areas. The spatial variation reflects the influence of basin topography on the differences in the precipitation spatial distribution.

The distribution of precipitation is affected by topography. The elevation change in the basin is complex, and the leeward slope varies a lot. Therefore, this has a significant impact on precipitation. Areas with less precipitation are at higher elevations and on mountain leeward slopes, and lack moist air flow. The area with more precipitation is to the summer monsoon mountain windward slope, and the topography blocks an increase in precipitation. The elevation of the central region is relatively uniform and the terrain is flat. Therefore, the distribution of precipitation is more uniform. The results can provide a reference for regional agricultural development and resource utilization, and contribute to the protection of the ecological environment.

References

1. Jehn, F.U.; Kemp, L. Focus of the IPCC Assessment Reports Has Shifted to Lower Temperatures. *Earths Future* **2022**, *10*, e2022EF002876. [CrossRef]
2. Liu, P.R.; Raffery, A.E. Country-based rate of emissions reductions should increase by 80% beyond nationally determined contributions to meet the 2 °C target. *Commun. Earth Environ.* **2021**, *2*, 29. [CrossRef] [PubMed]
3. Lenton, T.M.; Rockstorm, J. Climate tipping points–too risky to bet against. *Nature* **2019**, *575*, 592–595. [CrossRef] [PubMed]
4. Koutsoyiannis, D. Climate change, the Hurst phenomenon, and hydrological statistics. *Hydrol. Sci. J.* **2013**, *48*, 3–24. [CrossRef]
5. Fabio, D.N.; Marco, D.M. A Combined Clustering and Trends Analysis Approach for Characterizing Reference Evapotranspiration in Veneto. *Sustainability* **2023**, *15*, 11091–11114.
6. Stefanos, S.; Dimitrios, S. Spatial and Temporal Rainfall Variability over the Mountainous Central Pindus (Greece). *Climate* **2018**, *6*, 75–90. [CrossRef]
7. Chauhan, A.S.; Singh, S. Spatio-temporal and trend analysis of rain days having different intensity from 1901–2020 at regional scale in Haryana, India. *Results Geophys. Sci.* **2022**, *10*, 100041. [CrossRef]
8. Gu, X.H.; Zhang, Q. Evaluation on Stationarity Assumption of Annual Maximum Peak Flows during 1951–2010 in the Pearl River Basin. *J. Nat. Resour.* **2015**, *30*, 824–835.
9. Yin, Y.X.; Chen, H.S. Modeling Extreme Precipitation in the Poyang Lake Basin Based on Stationary and Non-stationary GEV Models. *J. Nat. Resour.* **2016**, *31*, 1906–1917.
10. Song, T.Y.; Chen, Y. Temporal and spatial variation and non-stationary characteristics of extreme precipitation in the Shanmei reservoir basin. *South North Water Transf. Water Sci. Technol.* **2022**, *20*, 327–337.
11. Kong, F.; Fang, J.Y. Variations in the spatiotemporal patterns of precipitation concentration degree and precipitation concentration period from 1951 to 2012 in China. *J. Beijing Norm. Univ.* **2015**, *51*, 404–411.
12. Wang, W.; Li, Z.Y. The Characteristics of Precipitation Concentration Degree over Jiangsu Province in 1961–2014. *Meteology Disaster Reduct. Res.* **2018**, *41*, 36–43.
13. Wang, M.X.; Yan, J.P. Spatial-temporal Variation of Intra-annual Precipitation Concentration Degree and Precipitation Concentration Period on Southeast Coast of China from 1960 to 2013. *Bull. Soil Water Conserv.* **2016**, *36*, 277–287.
14. Li, Y.J.; Yan, J.P. Relationship between Dryness/Wetness and Precipitation Heterogeneity in the North and South of the Qinling Mountains. *Arid. Zone Res.* **2016**, *33*, 619–627.
15. Zhou, G.L.; Dai, S.B. Spatial and temporal variation characteristics of heavy rainfall in the Huaihe River Basin in recent 60 years. *South North Water Transf. Water Sci. Technol.* **2015**, *13*, 847–852.
16. Huang, X.Y.; Chen, X. Analysis of Daily Rainfall Concentration and Its Change Characteristics in Southwestern Karst Regions-A Case Study of Wujiang Catchment. *Earth Environ.* **2013**, *41*, 203–208.
17. Pang, X.X. Inter-annual Variations of Precipitation Concentration Degree and Concentration Index in Huaihe River Basin. *J. Yangtze River Sci. Res. Inst.* **2018**, *35*, 43–47.
18. Li, Y.P.; Yang, T.B. Change Characteristics of Precipitation Concentration Degree (PCD) and Precipitation Concentration Period (PCP) in the Flood Season in Pi River Valley. *Resour. Sci.* **2012**, *34*, 418–423.
19. Xia, Z.B.; Huang, Y.M. Temporal and spatial pattern of daily rainfall concentration in the middle and upper reaches of Hanjiang River Basin. *Yangtze River* **2020**, *51*, 76–79.
20. Li, B.; Li, L.J. Changes in Precipitation Extremes in Lancang River Basin in 1960–2005. *Prog. Geogr.* **2011**, *30*, 290–298.
21. Dong, M.Y.; Wang, L.Q. Spatial-temporal variations in intra-annual precipitation concentration degree and precipitation concentration period in Luanhe River Basin from 1960–2017. *Prog. Geogr.* **2011**, *30*, 290–298.

22. Cao, Y.X.; Cai, H.K. Characteristics of Precipitation Concentration Index Variations in Southwest China from 1963 to 2012. *J. Southwest Univ. (Nat. Sci. Ed.)* **2016**, *38*, 117–124.
23. Liu, X.F.; Ren, Z.Y. Inhomogeneity Characteristics of Intra-annual Precipitation on the Loess Plateau during 1959–2008. *Prog. Geogr.* **2012**, *31*, 1157–1163.
24. Hu, L.L.; Li, L.P. Precipitation Concentration Degree and Precipitation Concentration Period in the East Hexi Corridor in Flood Season. *Arid. Zone Res.* **2016**, *33*, 758–765.
25. Gao, H.M.; Yan, X.D. Analysis on Climatic characteristics of precipitation in Wujiang River Basin in recent 50 years. In Proceedings of the 2013 Annual Meeting of Guizhou Meteorological Society, Anshun, China, 19 November 2013.
26. Xiong, Y.L.; Zhang, K.L. Periodic Changes of the Precipitation and Runoff in Wu River Watershed. *J. Sichuan Agric. Univ.* **2010**, *28*, 475–479.
27. Ji, T.Y.; Hu, Y.W. Analysis of the strong Rainfall Weather Characteristics in Wujiang River Based on the Latest Observation Data. *J. Anhui Agri. Sci.* **2014**, *41*, 11415–11419.